

Received July 6, 2017, accepted July 22, 2017, date of publication September 1, 2017, date of current version February 1, 2018.

Digital Object Identifier 10.1109/ACCESS.2017.2741220

# You Can Recharge With Detouring: Optimizing Placement for Roadside Wireless Charger

XUNPENG RAO<sup>1</sup>, YUBO YAN<sup>1</sup>, (Student Member, IEEE),  
MAOTIAN ZHANG<sup>1</sup>, (Student Member, IEEE), WANRU XU<sup>1</sup>,  
XIAOCHEN FAN<sup>2</sup>, HAO ZHOU<sup>3</sup>, (Member, IEEE),  
AND PANLONG YANG<sup>3</sup>, (Member, IEEE)

<sup>1</sup>College of Communications Engineering, PLA University of Science and Technology, Nanjing 210007, China

<sup>2</sup>FETT, School of Computing and Communications, University of Technology Sydney, Sydney, NSW 2007, Australia

<sup>3</sup>School of Computer Science and Technology, University of Science and Technology of China, Hefei 230026, China

Corresponding author: Panlong Yang (panlongyang@gmail.com)

This work was supported in part by NSF of Jiangsu for Distinguished Young Scientist under Grant BK20150030; in part by NSFC under Grant 61632010, Grant 61232018, Grant 61371118; in part by the China National Funds for Distinguished Young Scientists under Grant 61625205; in part by the Key Research Program of Frontier Sciences, CAS, under Grant QYZDY-SSWJSC002, Grant 61402009, Grant 61672038, Grant 61520106007; and in part by NSF under Grant ECCS-1247944, Grant NSF CMMI 1436786, and Grant NSF CNS 1526638.

**ABSTRACT** Wireless energy transfer technologies have played an important role in the development of Internet of Things. Most of the previous studies focus on scheduling mobile chargers efficiently for rechargeable sensor nodes. In this paper, we investigate the deployment problem for wireless charging stations (WCSs) in urban areas with respect to the users detouring cost when they move to the candidate WCSs. With pre-known user's trajectories and given number of WCSs, we deploy the WCSs to maximize the number of recharged users with guaranteed probability. We convert our deployment problem into an NP-hard weighted maximum coverage problem, and prove the objective function is a maximum submodular set function. To this end, a simple but efficient greedy algorithm with approximation factor of  $(1 - \frac{1}{e})$  is proposed for the threshold detouring mode. In addition, an improved algorithm with an approximation factor of  $(1 - \frac{1}{\sqrt{e}})$  is presented for the linear/nonlinear detouring mode. Finally, we evaluate the performance of our algorithms by comparing them with two typical heuristic algorithms (*flow-centric* and *random-based*), and the impacts of different detouring thresholds on our algorithms by synthetic traces. Moreover, real trace-driven evaluations validate that our algorithm improves the coverage quality by 75% when compared to the two aforementioned algorithms.

**INDEX TERMS** Wireless energy transfer, charger placement, detour, approximation algorithm.

## I. INTRODUCTION

### A. BACKGROUNDS AND MOTIVATION

With the rapid growth of wireless sensor networks (WSNs) [1]–[3], energy conservation studies have attracted more and more attentions from academic and industrial domain [4], [5]. To address the capacitated energy problem, some energy conservation protocols had been proposed [6], [7]. However, these methods are insufficient for long-term deployment and maintenance in WSNs. Recently, some studies [8] of harvesting ambient energy have been investigated to empower sensors, such as solar energy, wind energy, electromagnetic radiation. But the ambient energy sources are unpredictable and intermittent, which causes that the harvesting energy is not always available. Particularly, wireless energy transfer technology [9] can provide the steady and controllable

energy source. Based on wireless power transfer, there have been many available purchased commercial and promising products in markets, such as sensors [10] and powermat [11]. Although it has attracted increasing attention due to the advantage without requiring the charging cable, whereas no less than an hour of long recharging time is required for a typical sensor node equipped with traditional NiMH battery, which lowers the user-experience especially in large-scale WSNs. To address the issue, the ultra fast charging technology has been proposed to promote the feasibility of wireless power transfer, which can achieve 400 *Coulombs* per second recharging efficiency based on material *LiFePO<sub>4</sub>* [12], *i.e.*, a few seconds to fully recharge a typical sensor node. Therefore, wireless power transfer technology is a promising method to extend the lifetime of WSNs.

Most of previous work [13]–[16] in wireless rechargeable sensor network focus on scheduling mobile chargers with different optimal objectives, such as maximizing the lifetime of network or minimizing the charging delay. On the other hand, the studies of placement problems for stationary chargers are few relatively. Zhang *et al.* [17] studied the joint optimization of charger deployment and power allocation to maximize the charging quality. Moreover, Dai *et al.* investigated the chargers' placement considering electromagnetic radiation safety issue [18]. However, both of the studies focused on finding optimal placement scheme for static rechargeable nodes. The case of mobile nodes hasn't been studied in wireless charger placement. In smart urban city, many studies have been investigated on the placement of charging stations for electric vehicles (EVs). Xiong *et al.* [19] considered EVs drivers' strategic behaviors caused by traffic condition and queuing time to minimize the charging cost. Hess *et al.* [20] introduced a mobility model with state changing scheme between regular mobility state and detouring state to minimize the average trip time. However, none of these work capture the interrelationship between charging demand and detouring expectation (a kind of description to the degree of detouring desire to users, which will be formally addressed in Sec. IV-B) caused by detouring distance. Moreover, J. Walker's work [21] explores the threshold effects of detouring distance for human between bus and subway stations on placement of stations. Inspired by this vision, we investigate whether or not the charging demand is affected by detouring distance. As mentioned in [22], the detouring distance would affect the personal desire, *i.e.*, most of participants would accept the detouring distance within a threshold, while desire changing may occur if the detouring distance exceeds the threshold. It indicates that the detouring expectation is non-increasing with the increased detouring distance. In addition, the tradeoff between detouring cost and recharging demands should be concerned carefully.

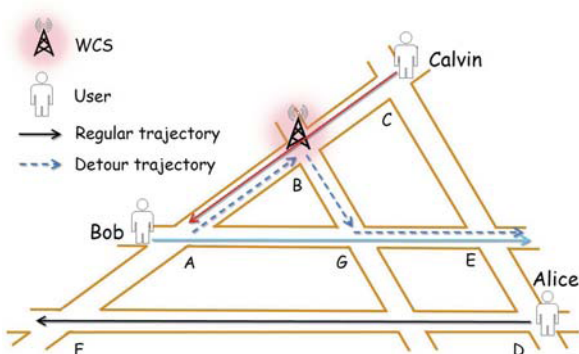


FIGURE 1. Scenario of wireless charging station placement.

An illustrative example is shown in Fig. 1, Bob, Alice and Calvin are traveling along the flow  $AE$ ,  $DF$  and  $CA$  respectively, which are depicted with solid lines, and a WCS is placed at the intersection  $B$ . In that, Calvin doesn't need any

additional detouring cost, because the WCS is on the way of his regular flow. On the contrary, both Bob and Alice need detour to the intersection  $B$  because the WCS is not listed in their flows. The detouring path for Bob has been shown in the figure with dotted lines. Meanwhile, we notice that the detouring distance of Alice is much longer than Bob's, which means she possibly gives up detouring to the WCS.

In this paper, we consider the placement optimization problem for WCSs, respecting the detouring cost in urban area. In that, the WCSs are usually deployed at the intersections and the users are traveling along the regular trajectories. As for this kind of system, the WCSs' locations are publicly known to users by using smartphone with MCPS [23]. If the WCSs are not deployed on users' regular trajectories, users may detour to WCSs for recharging their phones or smart devices depending on the detouring distance. To this end, we investigate the detouring effects in our model and make comprehensive evaluations on it.

Given users' trajectories and a number of WCSs, we focus on optimizing the WCSs deployment to cover maximum users. With convincing analyses in Sec. V-B, it turns out that our deployment problem is a weighted maximum coverage problem [24], which has been proved to be NP-hard. By reducing from maximum coverage problem, our maximum coverage quality with threshold mode is 0/1 coverage problem. Therefore, a simple but efficient threshold mode-driven algorithm is proposed with guaranteed performance by leveraging the favorable properties of submodular optimization [25], which has been presented as preliminary study [26]. Moreover, we notice that the decreasing property of linear/nonlinear detouring modes makes our coverage problem become non-0/1 coverage. Based on an improvement in threshold mode-driven algorithm, we propose the linear/nonlinear mode-driven algorithm and prove the approximation ratio. As users density and detouring cost of different trajectories are significantly different, the challenge of placing WCSs comes from the tradeoff between users density and the detouring cost. Furthermore, the effects of detouring threshold and different detouring modes make our problem more challenging. Finally, we conduct extensive evaluations to evaluate the performance of our algorithms comparing with two typical heuristic algorithms. One is *flow-centric*, which places WCSs at the top- $k$  intersections ranked by the number of covered trajectory flows. Another one is *random-based* scheme which provides a good baseline scheme for evaluation. Moreover, the evaluations based on real-world traces [27] validate that the proposed algorithms improve coverage quality by 75% comparing with two aforementioned algorithms.

## B. CONTRIBUTIONS

In summary, our contributions could be summarized as follows:

- We consider a placement scheme for roadside wireless chargers with bounded detouring cost. And we present the maximum coverage quality problem with limited

WCSs by reducing from weighted maximum coverage problem. To handle this NP-hard problem, we proved the submodularity of our objective function. To this end, an simple but efficient greed algorithm with ratio of  $(1 - \frac{1}{e})$  is proposed for threshold detouring mode.

- We notice that the difference caused by decreasing detouring expectation of linear/nonlinear mode would make our problem be more complicated than above coverage problem. Then, we propose an improvement by reconsidering the covered flows in previous greedy stages and prove that the approximate ratio could be up to  $(1 - \frac{1}{\sqrt{e}})$  to the optimal solution for the decreasing linear/nonlinear detouring mode.
- Extensive experiments are conducted to evaluate the proposed algorithms by comparing with two typical heuristic algorithms (*flow-centric* and *random-based*). Based on the synthetic traces, we investigate the effects of different parameters on performance of the proposed algorithms. Furthermore, by real-world traces, it shows that our algorithms also outperform the typical heuristic algorithms by 75%, and the improvement gap is significant with the increased detouring thresholds.

### C. PAPER ORGANIZATION

The remainder of this paper is organized as follows. In Sec. II, we give a survey of wireless charger placement and mobile charger scheduling. Before modelling network and detour models in Sec. IV, we introduce preliminaries in Sec. III. In Sec. V, we formulate our problem. And threshold and linear/nonlinear mode-driven algorithms are proposed. In Sec. VI, we conduct extensive evaluations and show the results with comprehensive analyses. Finally, we conclude our work in Sec. VII.

## II. RELATED WORK

### A. WIRELESS STATIONARY CHARGER PLACEMENT

The stationary wireless charger placement problems [17], [18], [28]–[30] sought to find placement schemes for stationary chargers to replenish batteries for sensor nodes. These studies were made by proposing different optimization objectives and application scenarios, deploying constraints.

In Zhang's work [17], a charger placement with variable power levels and budgets was concerned carefully. In that, the chargers were deployed by an approximation algorithm with approximation factor of  $\frac{1-1/e}{2L}$  to maximize the number of all utilized charging power of nodes. Dai *et al.* [28] proposed a placement scheme for energy sources to optimize the cost-effective deployment. In that, only the one dimensionality spatial distribution of nodes was concerned. After that, in a given charger placement, H. Dai *et al.* proposed another near optimal scheme about how to find the maximum electromagnetic radiation point [29]. Moreover, the issues of electromagnetic radiation safety and capacity constraints on charger placement had been taken into consideration [18] [30].

### B. WIRELESS MOBILE CHARGER SCHEDULING

The mobile charger scheduling problems [13], [14], [31]–[33] had been studied to seek optimal traveling paths or collaborative recharging scheme with different scenarios and optimizing objectives.

Shi *et al.* [13] proposed an periodic recharging scheme to service all nodes with maximizing the ratio of vacation time in service station over a recharging cycle time. This work was extended to recharging multi-node simultaneously with the same optimal objective [14]. Given a budget (*e.g.*, time or energy), Chen *et al.* [31] sought to find an optimal traveling path for charger to maximize the number of rechargeable mobile nodes. Zhang and Wu [32] proposed an optimal collaborate recharging scheme for multi-charger scheduling, where the mobile chargers can recharge each other to service a larger area. Xu *et al.* [33] investigated the different frequencies of recharging demand, and studied how to schedule multi-chargers to service multiple recharging cycles with minimizing the total traveling cost.

These studies on mobile chargers could increase the controllability of charging assignment and provide the solutions for the inflexibility of stationary charger placement. Based on the energy-efficient data-gathering in WSNs [34], it is worth to investigate the joint optimization of data gathering or transmission and energy recharging in wireless rechargeable sensor network [35], [36]. Specifically, although advanced algorithms have been proposed to solve aforementioned difficulty [37], [38], they could not be applicable to our investigation due to the joint complexity on both placement and detouring.

## III. PRELIMINARIES

First of all, we introduce the preliminary definition of submodular set function [39] such that the favorable property in submodular optimization could be leveraged in our optimal deployment problem.

*Definition 1 (Submodularity):* Given a finite set  $\Omega$ , a real-valued function  $f(\cdot)$ , which is a set function  $f : 2^\Omega \rightarrow \mathbb{R}$  on the set of subsets of  $\Omega$ , is called submodular if it satisfies

$$f(\alpha) + f(\beta) \geq f(\alpha \cup \beta) + f(\alpha \cap \beta), \quad \forall \alpha, \beta \subseteq \Omega.$$

Firstly, the set function  $f(\cdot)$  is required to be nondecreasing, *i.e.*,  $f(\alpha) \leq f(\beta)$ ,  $\forall \alpha \subseteq \beta \subseteq \Omega$ .

Then, a formal definition of submodularity is that, the function satisfies the *diminishing returns* rule. That is, arbitrary  $\alpha \subseteq \beta \subseteq \Omega$  and  $u \in \Omega \setminus \beta$ , it holds that

$$\Delta(u|\alpha) \geq \Delta(u|\beta),$$

where  $\Delta(u|\alpha) = f(\alpha \cup \{u\}) - f(\alpha)$ . In other words, it is the utility contribution of adding an element  $u$  to a subset  $\alpha$  for set function  $f(\cdot)$  that is at least as large as the utility contribution of adding the same element to the subset  $\beta$ .

In addition, the related work about submodular function could be regarded as set function with convexity had been shown in Lovász's work [40].

TABLE 1. Annotations for frequently used symbols.

Symbol	Definition
$V$	The set of intersections
$T$	The set of trajectory flows
$W$	The set of number of users in $T$
$T_{ij}$	The flow from $i$ to $j$
$d_{ij}$	The length of $T_{ij}$
$w_{ij}$	The number of users in $T_{ij}$
$d_{ij}^{v_m}$	The detouring distance from $T_{ij}$ to $v_m$
$D$	The threshold value of detouring
$C_{v_m}$	The set of flows covered by $v_m$
$R_{v_m}(T_{ij})$	The state of $T_{ij}$ covered by $v_m$ or not
$U_{v_m}(T_{ij})$	The number of users in $T_{ij}$ covered by $v_m$

IV. SYSTEM MODEL

A. SCENARIO DESCRIPTION

We start with the scenario of an undirected graph  $G = (V, E)$ . In that,  $V$  is a set of vertexes (i.e., street intersections  $V = \{v_1, v_2, \dots, v_n\}$ ), and  $E$  is the set of undirected edges. The length of each edge in  $E$  is defined by Euclidean distance. As shown in Fig. 1, the WCSs are deployed at street intersections, which provide users' mobile devices with energy by wireless power transfer technologies.

There are some traffic flows existing on the streets, which consist of users' trajectories. For simplicity, we assume that all trajectories start from and end at intersections. Let  $T_{ij}$  denote the trajectory from intersection  $i$  to  $j$ , and the length of trajectory  $T_{ij}$  is denoted by  $d_{ij}$ . Generally, there are multi-paths from intersection  $i$  to  $j$ . In our work, the traveling path for flow  $T_{ij}$  is unique and known in priori, which is the shortest path. And we assume that users from intersection  $i$  to  $j$  would travel along flow  $T_{ij}$ . Let  $T$  denote the set of trajectory flows,  $T = \{T_{ij} | 1 \leq i, j \leq n\}$ , and  $W$  denote the set of number of users in trajectories daily,  $W = \{w_{ij} | 1 \leq i, j \leq n\}$ . WCSs' locations can be found by users' mobile phones. When users find the WCSs, users could choose and detour to one, which is depending on the detouring distance.

B. DETOUR MODEL

First of all, we assume that users in flow  $T_{ij}$  would travel along the shortest path to detour to a WCS from  $v_i$ . Let  $d_{ij}^{v_m}$  denote the detouring distance for users in flow  $T_{ij}$  detouring to intersection  $v_m$ , and it is given by

$$d_{ij}^{v_m} = d_{im} + d_{mj} - d_{ij}.$$

As depicted in Fig. 2, there are two candidate intersections  $v_1, v_2$  for WCS and three traveling paths. In that, the shortest length of flow  $T_{34}$  from  $v_3$  to  $v_4$  is denoted by  $d_0$ , which is shown by solid lines. Suppose a user in flow  $T_{34}$  decides to detour to the WCS deployed at  $v_2$ , the detouring distance  $d_{34}^{v_2}$  can be given by  $d_{34}^{v_2} = d_1 + d_2 - d_0$ , where  $d_1$  is the shortest path from  $v_3$  to  $v_2$ , and  $d_2$  is the shortest path from  $v_2$  to  $v_4$ .

Next, we introduce our utility function,  $f(d_{ij}^{v_m})$ , to describe the detouring expectation of users in flow  $T_{ij}$  detouring to  $v_m$ . As mentioned in [22], we observe that users may give up

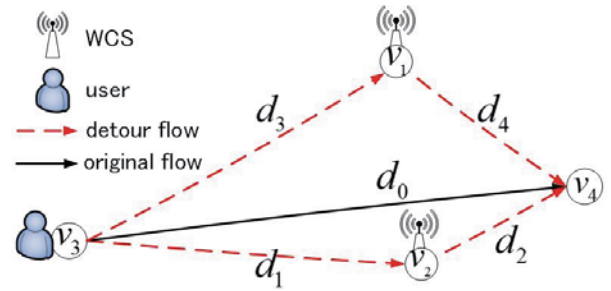


FIGURE 2. Detour model.

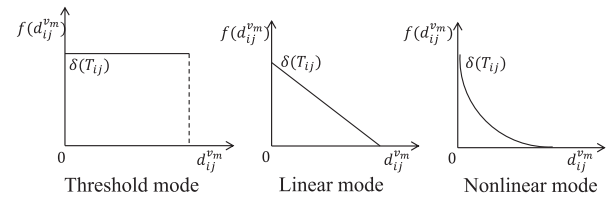


FIGURE 3. Three kinds of detouring modes.

detouring to a WCS if the detouring distance to the WCS is very large. That is to say, it is not cost-effective for users to spend too much detouring cost to recharge. Hence the detouring expectation is non-increasing with respect to the detouring distance. In Huanyang's work [41], the effects of detouring cost on attractiveness of advertisements have been studied carefully, and three kinds of detouring utility functions are presented to measure the detouring probability. As shown in Fig. 3, the identical three kinds of detouring utility functions are adopted to describe the detouring expectation corresponding to three kinds of different detouring patterns as follows:

1) THRESHOLD MODE

The detouring expectation maintains unchanged before detouring distance exceeding a given threshold, which is given by

$$f(d_{ij}^{v_m}) = \begin{cases} \delta(T_{ij}), & \text{if } d_{ij}^{v_m} \leq D \\ 0, & \text{otherwise} \end{cases} \quad (1)$$

In this mode, the detouring expectation is a certain constant within the threshold. This mode is used to focus on the impacts of detouring thresholds.

2) LINEAR MODE

The detouring expectation linearly decreases with the increased detouring distance before exceeding a given detouring threshold. This mode is presented by taking the changing process of detouring expectation into consideration. It is shown as

$$f(d_{ij}^{v_m}) = \begin{cases} \delta(T_{ij}) \cdot (1 - \frac{d_{ij}^{v_m}}{D}), & \text{if } d_{ij} \leq D \\ 0, & \text{otherwise} \end{cases} \quad (2)$$

The detouring expectation is decreasing linearly within the threshold in this mode. It is used to focus on the impacts of decreasing detouring expectation.

### 3) NONLINEAR MODE

The detouring expectation nonlinearly decreases with the increased detouring distance before exceeding a given detouring threshold. It is more practical to describe the nonlinear changing process than linear mode. It is defined as

$$f(d_{ij}^{v_m}) = \begin{cases} \delta(T_{ij}) \cdot (1 - \sqrt{\frac{d_{ij}^{v_m}}{D}}), & \text{if } d_{ij}^{v_m} \leq D \\ 0, & \text{otherwise} \end{cases} \quad (3)$$

The nonlinear decreasing of detouring expectation is applied in this mode, which is used to focus on describing the decreasing gradient changing by comparing to linear mode.

In these modes, the  $\delta(T_{ij})$  is the parameter to describe the degree of recharging demand (a number between 0 and 1) for the users in trajectory  $T_{ij}$ . The *linear mode* and *nonlinear mode* show that detouring expectation  $f(d_{ij}^{v_m})$  strictly decrease from  $\delta(T_{ij})$  to 0 with respect to detouring distance  $d_{ij}^{v_m}$ . And  $D$  is the detouring threshold value (i.e.,  $D$  is the maximum detouring distance). The number of users covered by  $v_m$ , who are willing to detour to the  $v_m$ , is calculated by  $f(d_{ij}^{v_m}) \cdot w_{ij}$ . For simplicity, we assume that a WCS can serve enough users (i.e., a WCS can serve numerous users).

### C. COVERAGE QUALITY

In this subsection, we introduce the concept of coverage set for flows, before defining the quality of the intersection in terms of coverage. We regard that a flow  $T_{ij}$  is covered by an intersection  $v_m$ , if and only if the corresponding detouring distance  $d_{ij}^{v_m}$  is no greater than  $D$ , i.e.,  $d_{ij}^{v_m} \leq D$ . Let  $R_{v_m}(T_{ij})$  denote whether an intersection  $v_m$  covers flow  $T_{ij}$  or not. The presentation of  $R_{v_m}(T_{ij})$  could be described as:

$$R_{v_m}(T_{ij}) = \begin{cases} 1, & \text{if } d_{ij}^{v_m} \leq D \\ 0, & \text{otherwise} \end{cases}$$

Therefore, the set of flows covered by the intersection  $v_m$  is  $C_{v_m} = \{T_{ij} | R_{v_m}(T_{ij}) = 1, T_{ij} \in T\}$ . For example in Fig. 2, if  $d_{34}^{v_2} \leq D$  and  $d_{34}^{v_1} \geq D$ , then we have  $R_{v_2}(T_{34}) = 1$  and  $R_{v_1}(T_{34}) = 0$ .

**Definition 2 (Coverage Quality):** Given a flow  $T_{ij}$  and a WCS  $v_m$ , the coverage quality of  $v_m$  on  $T_{ij}$  is the weight  $w_{ij}$  of  $T_{ij}$  covered by  $v_m$ , which is given by

$$U_{v_m}(T_{ij}) = f(d_{ij}^{v_m}) \cdot w_{ij} \cdot R_{v_m}(T_{ij}).$$

Then the coverage quality of  $v_m$  regarding all flows  $T$  is the sum of number of users covered by  $v_m$  in the flows set  $C_{v_m}$ , i.e.,

$$U_{v_m}(T) = \sum_{T_{ij} \in C_{v_m}} U_{v_m}(T_{ij}).$$

Finally, the total coverage quality of a set of intersections  $V'(V' \subseteq V)$  regarding all flows  $T$  is the sum of coverage

quality of  $v_m (v_m \in V')$  in terms of flows set  $\bigcup_{v_m \in V'} C_{v_m}$ , i.e.,

$$U_{V'}(T) = \sum_{T_{ij} \in \bigcup_{v_m \in V'} C_{v_m}} \sum_{v_m \in V'} U_{v_m}(T_{ij}).$$

Furthermore, it is worth noting that the users and flows could not be covered by two or more intersections in calculating the number of covered users. An example in Fig. 2, two WCSs are around the flow  $T_{34}$ , e.g.,  $v_1, v_2$ . If  $d_{34}^{v_2}, d_{34}^{v_1} \leq D$ , then  $R_{v_2}(T_{34}) = 1$  and  $R_{v_1}(T_{34}) = 1$ . When a WCS has been deployed at  $v_2$ , then the users in flow  $T_{34}$  would be covered by  $v_2$ . After this, when considering to deploy another WCS at  $v_1$ , the users in flow  $T_{34}$  could not be covered by  $v_1$  again. That is to say, the users and flows could not be counted repetitively.

## V. FORMULATION AND SOLUTION

### A. PROBLEM FORMULATION

**Definition 3 (Maximum Coverage Quality With Limited WCSs):** Given a set of  $n$  intersections  $V = \{v_1, v_2, \dots, v_n\}$  and flow set  $T = \{T_{ij} | 1 \leq i, j \leq n\}$  with weights  $W = \{w_{ij} | 1 \leq i, j \leq n\}$ , and a predefined number  $0 < k < n$ , the Maximum Coverage Quality with Limited WCSs is to find a subset  $V' \subseteq V$ , such that the total coverage quality  $U_{V'}(T)$  of subset  $V'$  is maximized under the condition of  $|V'| \leq k$ .

Formally, our optimization deployment problem is as follows:

$$\begin{aligned} & \max_{V' \subseteq V} U_{V'}(T) \\ & \text{subject to } |V'| \leq k \end{aligned}$$

### B. CONVERSION TO WEIGHTED MAXIMUM COVERAGE

The weighted maximum coverage problem is defined in [24] as follows. A collection of sets  $\mathbb{S} = \{S_1, S_2, \dots, S_n\}$  is defined over a domain element  $X = \{x_1, x_2, \dots, x_p\}$  with associated weights  $\{\omega_1, \omega_2, \dots, \omega_p\}$ . The task is to find a collection of sets  $S' \subseteq \mathbb{S}$ , such that the total weights of elements covered by  $S'$  is maximized, and the total number of subsets in  $S'$  wouldn't exceed a given number  $k$ .

Next, we are going to transform our problem into weighted maximum coverage problem without loss of generalization. Given a traffic flows set  $T$ , we first consider a single intersection  $v_m$  that covers a subset of flows  $C_{v_m} = \{T_{ij} | R_{v_m}(T_{ij}) = 1, T_{ij} \in T\}$ . Then a collection of coverage set for all intersections is  $\mathbb{C} = \{C_{v_1}, C_{v_2}, \dots, C_{v_n}\}$ . The coverage quality of each intersection is associated with the weights of flows covered by the intersection, in which a domain of elements (i.e., flow  $T = \{T_{ij} | 0 \leq i, j \leq n\}$ ). The number of users in a flow can be regarded as weight of the flow. The elements set  $X$  corresponds to the traffic flows set  $T$ , and the set  $\mathbb{S}$  corresponds to the set  $\mathbb{C}$ . Accordingly, the corresponding relationship between these two sets is

$$\mathbb{S} \rightarrow \mathbb{C}, X \rightarrow T.$$

The selection of a subset corresponds to selecting an intersection to deploy a WCS. It turns out that our deployment

problem is a weighted maximum coverage problem. Otherwise, the number of users in flow  $T_{ij}$  covered by  $v_m$  is calculated by  $f(d_{ij}^{v_m}) \cdot w_{ij}$ . Then the effects of bounded detouring cost would make our problem more different.

### C. SUBMODULARITY ANALYSIS

In this subsection, we are going to prove that the set function  $U_{V'}(T)$  is monotonously nondecreasing submodular, so that we can leverage the profitable property in submodular optimization.

*Proof:* Firstly, it is simply true that  $U_\phi(T) = 0$ . We consider  $V$ 's two arbitrary subsets  $S$  and  $S'$ , subject to  $S \subseteq S' \subseteq V$ . The covered traffic flows in subsets  $S$  and  $S'$  are  $\bigcup_{v_i \in S} C_{v_i} \subseteq \bigcup_{v_j \in S'} C_{v_j}$ . Accordingly, the covered quality is

$$U_S(T) \leq U_{S'}(T).$$

Therefore,  $U_{V'}(T)$  is monotonously nondecreasing.

Secondly, considering an arbitrary intersection  $u \in V \setminus S'$ , let  $\Delta_U(u|S) = U_{S \cup \{u\}}(T) - U_S(T)$  and  $\Delta_U(u|S') = U_{S' \cup \{u\}}(T) - U_{S'}(T)$ . When adding a user  $u$  into the subsets  $S$  and  $S'$ , the increased covered traffic flows are

$$\xi = \bigcup_{v_i \in S \cup \{u\}} C_{v_i} - \bigcup_{v_i \in S} C_{v_i}$$

and

$$\xi' = \bigcup_{v_j \in S' \cup \{u\}} C_{v_j} - \bigcup_{v_j \in S'} C_{v_j}$$

Since we have obtained that  $\bigcup_{v_i \in S} C_{v_i} \subseteq \bigcup_{v_j \in S'} C_{v_j}$ , and  $\bigcup_{v_i \in S \cup \{u\}} C_{v_i} \subseteq \bigcup_{v_j \in S' \cup \{u\}} C_{v_j}$  in a similar way. Since the traffic flows covered by intersection  $u$  may also covered by the intersections in subset  $S'$  or not. If the flows covered by  $u$  are not covered by intersections in subset  $S'$ , then we can get that  $\xi' = \xi$ . If some of flows covered by  $u$  are also covered by some intersections in subset  $S'$ , then we can get  $\xi' \subset \xi$ . Therefore, we have  $\xi' \subseteq \xi$ . Thus the relationship of the increased covered users by adding an intersection  $u$  to the subset  $S$  and  $S'$  is  $U_u(C') \leq U_u(C)$ . Then, we can get

$$\Delta_U(u|S') \leq \Delta_U(u|S),$$

which satisfies with the decreasing return rule [42], [43]. Therefore  $U_{V'}(T)$  is submodular. ■

To conclude, the  $U_{V'}(T)$  is monotonously nondecreasing submodular.

### D. THRESHOLD MODE-DRIVEN ALGORITHM

With submodular property of objective function [44], it has shown that the weighted maximum coverage problem has a greedy algorithm that can achieve a ratio of  $(1 - \frac{1}{e})$  in [45]. The algorithm uses enumeration technique partially and then leverages greedy selection scheme. In each iterative step, we select the set which can acquire the total weights maximized from the candidate sets. Otherwise, the traditional

### Alg-DM 1: Algorithm of Maximum Coverage Quality With Limited WCSs for Threshold Mode

**Input:** City graph  $G = (V, E)$ , intersections set  $V$ , traffic flows set  $T$  and weighted  $W$ , a number  $k$ .

**Output:** The selected intersections set  $V'$ , number of users covered.

```

1   $T^U = T; V' = \phi;$ 
2  for  $q = 1, q \leq k, q++$  do
3      for  $v_m$  in  $V \setminus V'$  do
4           $U_{v_m}(T) = \sum_{T_{ij} \in T^U} w_{ij} \cdot R_{v_m}(T_{ij}) \cdot f(d_{ij}^{v_m});$ 
5      end
6       $v_q = \arg \max_{v_m \in V \setminus V'} U_{v_m}(T);$ 
7      add  $v_q$  into  $V'$ ;
8      remove  $v_q$  from  $V$ ;
9      remove  $C_{v_q}$  from  $T^U$ ;
10 end

```

maximum coverage problem is 0/1 coverage problem in terms of elements. By reducing from maximum coverage problem, our maximum coverage quality with threshold mode is 0/1 coverage problem in terms of trajectories. Inspired by this observation, an approximation algorithm is proposed to solve our WCS deployment problem by using threshold mode.

As shown in Alg-TM. 1, mark all flows as uncovered in line 1, and the goal set  $V'$  is empty. Each iteration of the procedure is shown from line 3 to 9. From line 3 to 5, we compute the number of covered users from uncovered trajectories by each intersection which is not in  $V'$ . Then we select the intersection  $v_q$  which the number of covered users is maximum, and add this intersection  $v_q$  into the goal set  $V'$ . After that, from line 8 to 9, mark the flows covered by  $v_q$  as covered and remove the  $v_q$  from intersection set  $V$ . The  $k$ -iteration can be a repetition from line 3 to 9.

As description above, we iteratively deploy a WCS at an intersection, which can cover maximum users from uncovered trajectories. In that, the density of WCSs can be controlled well, since the flows covered are no longer considered in the next iterative step. It is obvious that the Alg-TM. 1 complexity is  $O(|V|^3)$ . The  $|V|$  is the number of intersections.

### E. LINEAR/NONLINEAR MODE-DRIVEN ALGORITHM

In last subsection, the maximum coverage quality is 0/1 coverage problem by considering threshold mode. For the computation pattern of  $f(d_{ij}^{v_m}) \cdot w_{ij}$ , the coverage quality is affected by detouring modes, which would make our problem more different. As the decreasing property of linear/nonlinear mode with the increased detouring distance, it makes the maximum coverage quality problem become a non-0/1 coverage problem. In this subsection, we investigate the maximum coverage quality problem by considering linear/nonlinear mode.

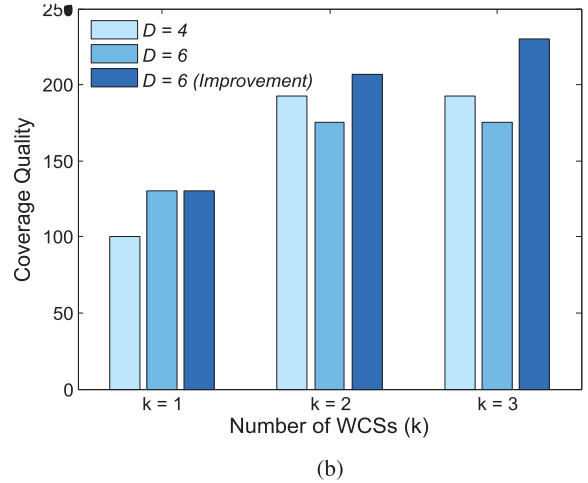
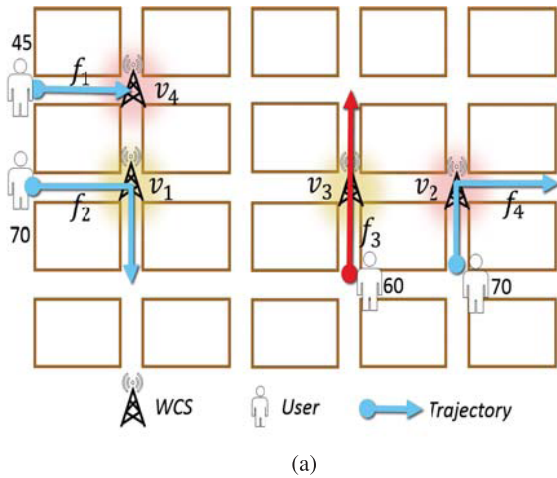


**FIGURE 4.** Example that presents the threshold mode-driven algorithm Alg-TM. (a) Roadmap of example. (b) Coverage Quality in Fig. 4a with linear mode.

First, we evaluate the proposed Alg-TM. 1 driven by threshold mode with an example in Fig. 4a.

1) EVALUATION SETTING

the graph is made by grid streets and the distances between two neighboring intersections are set to be 1. In that, there are four trajectories  $\chi = \{f_1, f_2, f_3, f_4\}$ . And the number of users in these trajectories are 45,70,60,70 respectively. Given  $k = 3$  WCSs, we conduct our evaluation in this example with two thresholds  $\{4, 6\}$ . The results is shown in Fig. 4b.

2) k = 1

the coverage quality with  $D = 6$  is greater than case of  $D = 4$ . It is obvious that the greater threshold  $D$  means the greater detouring expectation in linear/nonlinear mode.

(a)  $D = 4$ : by maximizing the covered users from uncovered trajectories, the first selected intersection is  $v_2$ . The coverage quality is  $U_{\{v_2\}}\{f_3, f_4\} = 70 + 60 \times \frac{2}{4} = 100$ .

(b)  $D = 6$ : the first selected intersection is  $v_3$ . The coverage quality is  $U_{\{v_3\}}\{f_2, f_3, f_4\} = 70 \times \frac{2}{6} + 70 \times \frac{4}{6} + 60 = 130$ .

3) k = 2

the coverage quality with  $D = 4$  outperforms the case of  $D = 6$ .

(a)  $D = 4$ : the second selected intersection is  $v_1$ . The coverage quality is  $U_{\{v_1\}}\{f_1, f_2\} + U_{\{v_2\}}\{f_3, f_4\} = 70 + 45 \times \frac{2}{4} + 100 = 192.5$ .

(b)  $D = 6$ : the second selected intersection is  $v_4$ . The coverage quality is  $U_{\{v_3\}}\{f_2, f_3, f_4\} + U_{\{v_4\}}\{f_1\} = 130 + 45 = 175 < 192.5$ .

Then a significant realization should be noticed is that the lower coverage quality by using linear mode with the greater detouring threshold  $D$ . As we know, the detouring expectation decreases with respect to detouring distance in linear/nonlinear mode. Thus, the coverage quality of overlapping regions is affected by different detouring distance.

In summary, the Maximum Coverage Quality Problem is not 0/1 coverage problem by using linear/nonlinear mode.

In the example above, the overlapping region is trajectory  $f_2$ . When  $D = 6$ , we could gain more covered users if  $f_3, f_4$  are covered by  $v_3$  in first iteration and  $f_1, f_2$  are covered by  $v_4$  in second iteration, that is  $U_{\{v_3\}}\{f_3, f_4\} + U_{\{v_4\}}\{f_1, f_2\} = 60 + 70 \times \frac{4}{6} + 70 \times \frac{4}{6} + 45 = 198.3 > 192.5$ . The reason is the  $v_4$  can offer a smaller detouring distance for  $f_2$  in second iteration than the first iteration. The smaller detouring distance means the greater detouring expectation which generates greater coverage quality. The improvement with  $D = 6$  is depicted in Fig. 4b.

This improvement shows that the trajectories which had been covered in previous iterations should be taken into consideration in later iterations. The observation is that the selected WCSs in later iterations would probably provide the shorter detouring distance for some trajectories than before, which had been covered in previous iterations. Inspired by this observation, we propose the linear/nonlinear mode-driven Alg-DM. 2. In that, each iteration consists of three steps. The first step is similar to Alg-TM. 1, that it finds the one which can cover maximum users from uncovered trajectories. The number of covered in the first step is marked as  $S$ . In the second step, it searches the one which can cover maximum additional users from covered trajectories in previous iterations from line 6 to line 10 shown in Alg-DM. 2. And the increased amount of users in the second step is denoted by  $S'$ . Then, compare  $S$  with  $S'$  in the third stage and select the maximum one. Similar to Alg-TM. 1, the deployment density of WCSs would be controlled well, since the greedy iteration is conducted by selecting the one which can provide with shorter detouring distance than before in the second step of Alg-DM. 2. In term of time complexity, it is same with Alg-TM. 1 that is  $O(|V|^3)$ , because the second step and first step are coordinative relation rather than possessive relation.

**Alg-DM 2:** Algorithm of Maximum Coverage Quality With Limited WCSs for Linear/Nonlinear Mode

**Input:** City graph  $G = (V, E)$ , intersections set  $V$ , traffic flows set  $T$  and weighted  $W$ , a number  $k$ .

**Output:** The selected intersections set  $V'$ , number of users covered.

```

1  $T^U = T; V' = \phi;$ 
2 for  $q = 1, q \leq k, q++$  do
3   for  $v_m$  in  $V \setminus V'$  do
4      $U_{v_m}(T) = \sum_{T_{ij} \in T^U} w_{ij} \cdot R_{v_m}(T_{ij}) \cdot f(d_{ij}^{v_m});$ 
5   end
6    $S = \max_{v_m \in V \setminus V'} U_{v_m}(T);$ 
7   for  $v_m$  in  $V \setminus V'$  do
8      $U'_{v_m}(T) = \sum_{T_{ij} \in T \setminus T^U} w_{ij} \cdot R_{v_m}(T_{ij}) \cdot f(d_{ij}^{v_m});$ 
9   end
10   $S' = \max_{v_m \in V \setminus V'} U'_{v_m}(T);$ 
11   $v_q = \arg \max_{v_m \in V \setminus V'} \{S, S'\}$ 
12  add  $v_q$  into  $V'$ ;
13  remove  $v_q$  from  $V$ ;
14  remove  $C_{v_q}$  from  $T^U$ ;
15 end

```

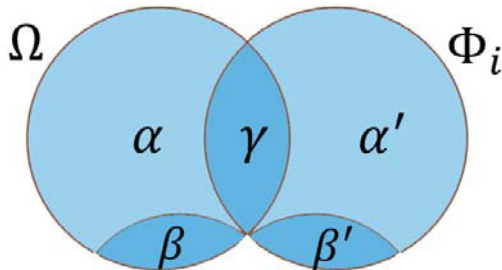


FIGURE 5. Set relationship.

By the design of improvement, we have the following theorem to describe the approximate ratio of Alg-DM. 2.

*Theorem 1:* The approximate ratio of Alg-DM. 2 could be up to  $(1 - \frac{1}{\sqrt{e}})$  comparing to the optimal solution, with respect to coverage quality of users.

*Proof:* Given  $K$  WCSs, let  $\Omega$  denote the optimal deployment, and  $\Phi_i$  denote the deployment acquired by Alg-DM. 2 after  $i^{th}$  iteration. Therefore,  $\Omega$  contains  $K$  WCSs and  $\Phi_i$  includes  $i$  WCSs. Then the coverage quality of users of  $\Omega$  and  $\Phi_i$  can be denoted by  $U(\Omega)$  and  $U(\Phi_i)$  respectively. As shown in Fig. 5, the coverage quality  $U(\Phi_i)$  is denoted by blue circle, and  $U(\Omega)$  is denoted by red circle.  $\alpha$  is the coverage quality by  $\Omega$  which are uncovered by  $\Phi_i$ . Similarly,  $\alpha'$  is the covered quality by  $\Phi_i$  which are uncovered by  $\Omega$ . Otherwise, there are some flows  $f$  which are both covered by  $\Omega$  and  $\Phi_i$ . The flows  $f$  can be divided into three parts, which are  $f_0, f_\Omega, f_{\Phi_i}$ .

Firstly,  $f_0$  is the flow that meet the rule of coverage quality  $U_\Omega(f_0) = U_{\Phi_i}(f_0) = \gamma$ . Then  $f_\Omega$  is the flows that meet the rule

of coverage quality  $U_\Omega(f_\Omega) > U_{\Phi_i}(f_\Omega)$ . Lastly,  $f_{\Phi_i}$  is the flows that meet the rule of coverage quality  $U_\Omega(f_{\Phi_i}) < U_{\Phi_i}(f_{\Phi_i})$ . Thus, the  $\beta, \beta'$  can be given by

$$\beta = U_\Omega(f_\Omega) - U_{\Phi_i}(f_\Omega)$$

and

$$\beta' = U_{\Phi_i}(f_{\Phi_i}) - U_\Omega(f_{\Phi_i}).$$

As shown in Fig. 5, we can get,

$$U(\Omega) = U(\Phi_i) - \alpha' - \beta' + \alpha + \beta.$$

Due to  $\alpha', \beta' \geq 0$ , then we have,

$$U(\Omega) \leq U(\Phi_i) + \alpha + \beta. \quad (4)$$

Next, we focus on the  $(i + 1)^{th}$  iteration of Alg-DM. 2. In the step one, the selected intersection is the one that can acquire maximum covered users from uncovered flows. With the greedy property, we can get the gain regressive of  $U(T_{i+1}) - U(T_i) \geq U(T_{i+2}) - U(T_{i+1})$ . Then we have,

$$\alpha \leq [U(\Phi_{i+1}) - U(\Phi_i)](K - i), \quad (5)$$

where  $(K - i)$  is the residue number of WCSs.

In the second step, it aims at finding the one that can gain maximum additional users from covered flows. Similarly, we have the gain regressive. Then we have

$$\beta \leq [U(\Phi_{i+1}) - U(\Phi_i)](K - i) \quad (6)$$

because the  $(K - i)$  gained maximum additional users from the covered flows should be no less than the additional users in  $\Omega$ .

Combining the Eq. 4 and Eq. 5, Eq. 6, we have

$$U(\Omega) - U(\Phi_i) \leq 2(k - i)[U(\Phi_{i+1}) - U(\Phi_i)]. \quad (7)$$

By conducting factorization in Eq. 7, we can get a recursive formulation as follows:

$$\begin{aligned}
 U(\Omega) - U(\Phi_i) &\geq \frac{2(K - i)}{2(K - i) - 1} [U(\Omega) - U(\Phi_{i+1})] \\
 &\geq \dots \\
 &\geq \left[ \frac{2(K - i)}{2(K - i) - 1} \right]^{K-i} [U(\Omega) - U(\Phi_K)].
 \end{aligned} \quad (8)$$

It is obvious that  $U(T_0) = 0$ . By setting  $i = 0$  in Eq. 8, we have

$$U(\Omega) \geq \left( \frac{2K}{2K - 1} \right)^K [U(\Omega) - U(\Phi_K)]. \quad (9)$$

It is well-known that  $\lim_{x \rightarrow \infty} (1 + \frac{1}{x})^x = e$ . By this extremum conclusion, we can get

$$U(\Omega) \geq \sqrt{e} [U(\Omega) - U(\Phi_K)]. \quad (10)$$

After that, Eq. 10 can be rewritten as

$$U(\Phi_K) \geq \left( 1 - \frac{1}{\sqrt{e}} \right) U(\Omega).$$

In summary, the approximate ratio of Alg-DM. 2 could be up to  $(1 - \frac{1}{\sqrt{e}})$ . ■



## VI. EVALUATION

In this section, we evaluate our proposed threshold mode-driven Alg-TM. 1 and linear/nonlinear mode-driven Alg-DM. 2 based on simulation traces and real-world traces. Moreover, we present the evaluation results and make analysis on it.

### A. COMPARISON ALGORITHMS AND METRICS

In our evaluation, two typical heuristic algorithms (namely *flow-centric* and *random-based*) are used for comparisons as follows:

(i) *Flow-centric*. It ranks the intersections by the number of covered trajectory flows. And then it places the WCSs at the top- $k$  intersections, which starts from the first one to  $k^{\text{th}}$  ranked according to the number of covered traffic flows.

(ii) *Random-based*. It places WCSs at the intersections uniformly.

We focus on the relationship between the number of WCSs and the ratio of covered users when considering different detouring modes, threshold  $D$ . The ratio of covered users is given by

$$\text{Ratio of covered users} = \frac{\text{Coverage Quality}}{\text{Total number of users}}$$

### B. EVALUATION BASED ON SIMULATION TRACE

#### 1) SIMULATION SETTING

We construct a roadmap  $G = (V, E)$  with  $|V| = 90$  intersections in a  $4500m \times 3000m$  square field. In that, we create a generator in Matlab to generate 180 traces randomly. In each trace, we use Matlab to generate [20,200] users randomly. We consider threshold values [200m,400m,600m,800m,1000m] to evaluate the effects of different coverage ranges of WCS on coverage quality. The parameter  $\delta(T_{ij})$  is set to be 1, because our WCSs are deployed to service for those users who are in need of recharging.

#### 2) SIMULATION RESULTS

Firstly, the primary concern in this evaluation is the performance of Alg-TM. 1 and Alg-DM. 2 by comparing with two typical heuristic algorithms (*flow-centric* and *random-based*). To this concern, we set the threshold value  $D = 600m$  in linear mode. As shown in Fig. 6, both the Alg-TM. 1 and Alg-DM. 2 outperform the *flow-centric* and *random-based* algorithms. In that, Alg-TM. 1 we proposed outperforms the *flow-centric* and *random-based* placement in terms of the ratio of covered users by at most 75% and 48% respectively. Furthermore, the performance improvement achieved by Alg-DM. 2 is significant compared to Alg-TM. 2. That is, Alg-DM. 2 outperforms Alg-TM. 1 by 17% in terms of ratio of covered users. And by the rising tendency of curves, the gap between Alg-DM. 2 and Alg-TM. 1 would be greater.

Another observation in Fig. 6 is that the *flow-centric* could acquire more users by comparing with *random-based* in incipient stage. After that, random based comes from behind with the increased number of WCSs. The reason

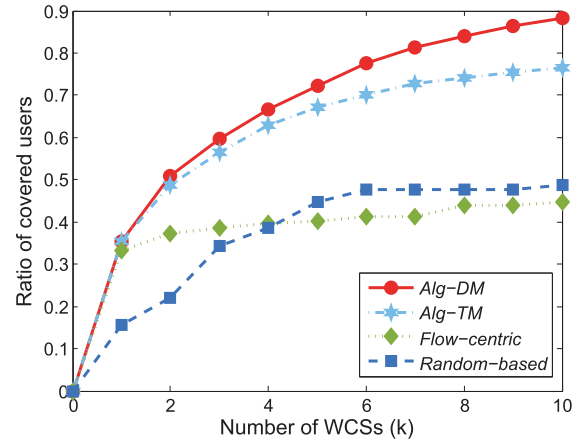


FIGURE 6. Ratio of covered users with the increased number of WCSs in linear mode. ( $D = 600m$ ).

is that *flow-centric* does not take the coverage overlapping region into consideration, which would result in the dense deployment. While for *random-based*, the dense deployment could be avoided for its uniform-randomness. Thus, random based would result in the less overlapping region than the *flow-centric*. Due to the computation definition of coverage quality, the users in overlapping region cannot be counted repeatedly. Therefore, random based would outperform *flow-centric* with the increased number of WCSs.

Then we evaluate the effects of different threshold values of detouring on coverage quality. In this part, the detouring mode (linear mode) remains unchanged. And the number of WCSs is 6 ( $k = 6$ ), three threshold values ( $D = 400m, 600m, 800m$ ) are concerned. Intuitively, the bigger the coverage range of WCS, the larger coverage quality. As shown in Fig. 8, the ratio of covered users achieved by Alg-DM. 2, *flow-centric* and *random-based* placement rises with the increased threshold value of detouring (coverage range) except the Alg-TM. 1, which follows the analysis in Sec. V-E. And that is the reason to propose improvement in Alg-DM. 2.

In Fig. 9, it shows that how the ratio of covered users acquired by Alg-DM. 2 changes as the joint increased number of WCSs and threshold value of detouring. In that, we can get that the ratio of covered users rises to the peak with increasing both number of WCSs ( $k$ ) and threshold value of detouring ( $D$ ). All the rising tendency in the two figures above can be explained in this figure.

### C. EVALUATION BASED ON REAL TRACE

#### 1) SIMULATION SETTING

In this subsection, the real trajectory data of bus traces in Seattle [27] would be used to conduct our evaluation. The bus traces consist of bus ID, x-coordinate, y-coordinate and route ID. For simplification, we focus on the traces within Seattle's center in an area of  $6km \times 6km$ . Some of real traces have been shown in Fig. 7b. According to the traces and Seattle's center roadmap of Fig. 7a, we set a city graph

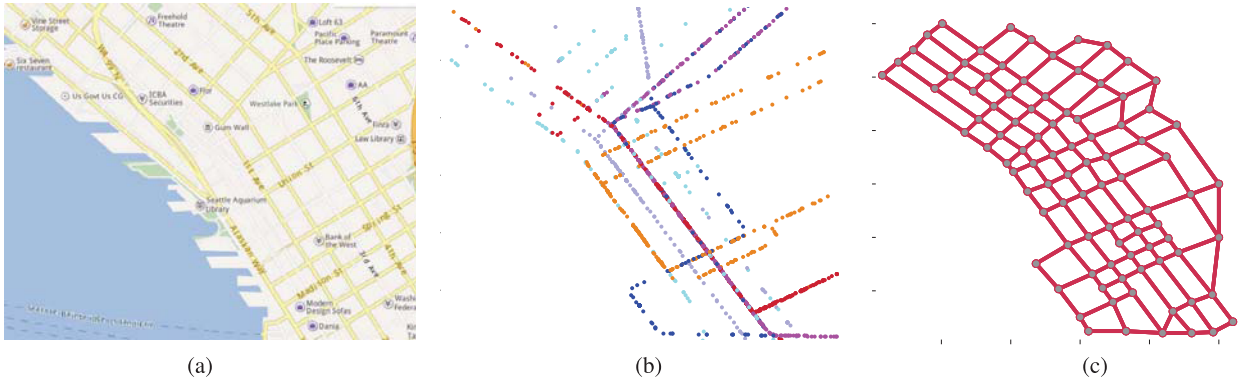


FIGURE 7. Real trace data in Seattle. (a) Seattle center roadmap. (b) Bus trajectory. (c) Our simulation graph.

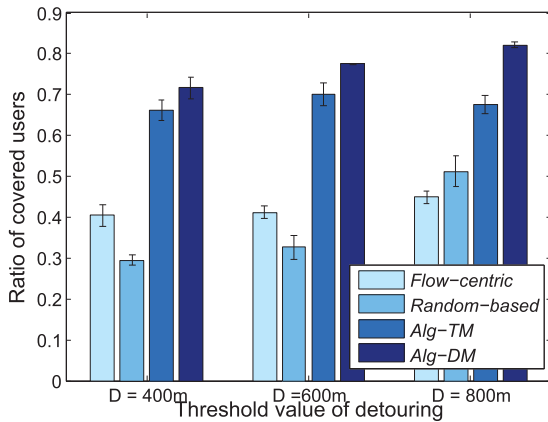


FIGURE 8. Ratio of covered users with different threshold values of detouring in linear mode. ( $k = 6$ ).

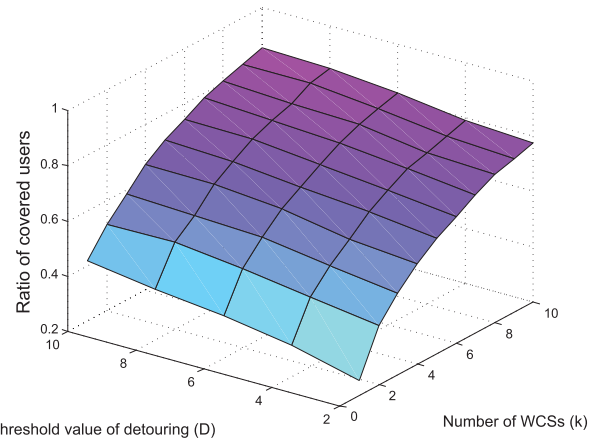


FIGURE 9. Joint effects of both number of WCSs and threshold of detouring  $D$  on the coverage quality in linear mode.

$G = (V, E)$  to represent the Seattle’s center roadmap approximately, which is depicted in Fig. 7c. In our evaluation, the routes are regarded as trajectories of users. For each trajectory, we use Matlab to generate [20, 200] users randomly.

Then, in this experiments, the three kinds of detouring modes are used. The first one is decreasing function  $i$  in linear mode. The second one and the third one are decreasing function in linear/nonlinear mode and threshold function in threshold mode. Under the same detour distance  $d_{ij}^m$  and the same threshold  $D$ , the detour probability of the threshold mode is the largest one, and linear mode is in the middle, nonlinear mode is the smallest one. Considering the scale of roadmap, we evaluation the impact of detouring threshold value by  $D = 400m, 800m, 1200m$ . For simplification,  $\delta(T_{ij})$  is set to be 1 for the same reason in the previous evaluation. Moreover, we would investigate the impact of this parameter on coverage quality in future work.

## 2) SIMULATION RESULTS

Firstly, we focus on the impacts of different detouring modes on coverage quality. As shown in Fig. 10, we conduct our algorithms by comparisons of linear mode, nonlinear mode and threshold mode with threshold  $D = 800m$ . It can be

seen that all algorithms could attract more users under the threshold mode. The reason is that the detour probability of threshold mode is the largest one comparing with the other two at the same detouring distance.

Otherwise, in Fig. 10b, the gap of ratio of covered users between Alg-TM. 1 and Alg-DM. 2 is the maximum one. It means that the coverage quality of nonlinear mode is less than linear mode, because the detouring probability of nonlinear mode is lower than linear mode.

In addition, the curves of Alg-DM. 2 and Alg-TM. 1 are coincident in Fig. 10c. In that, we can get that the Alg-DM. 2 would reduce to Alg-TM. 1 when considering the threshold utility function threshold mode. The reason is that our maximum coverage quality problem is a 0/1 coverage problem under the threshold mode, because the detouring probability value of threshold mode is 1 or 0.

Moreover, we explore the effects of different detouring thresholds  $D$  on the ratio of covered users with respect to number of WCSs. Before that, we introduce a metric to measure the improvement of algorithms we proposed. Given the selected subset of intersections and its coverage quality, the gap  $\psi$  is the difference value between  $R_1$  (ratio of covered users acquired by Alg-TM. 1) and  $R_2$  (ratio of covered users

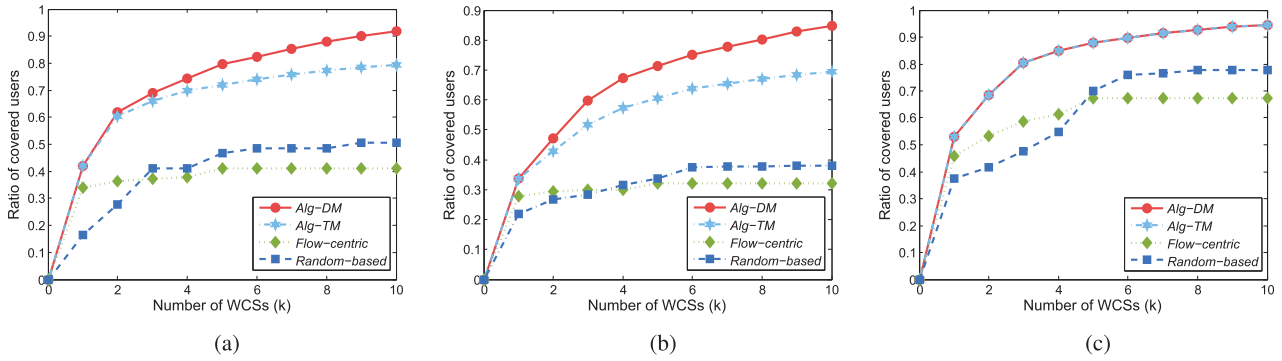


**FIGURE 10.** Ratio of users covered with the increased number of WCSs in different detouring mode ( $D = 800m$ ). (a) Ratio of covered users with the increased number of WCSs in linear mode. (b) Ratio of covered users with the increased number of WCSs in nonlinear mode. (c) Ratio of covered users with the increased number of WCSs in threshold mode.

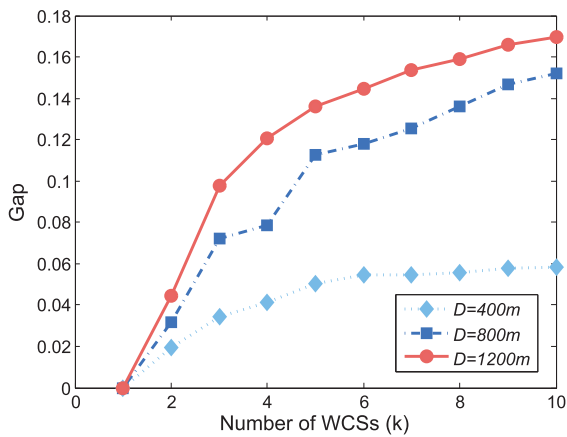


**FIGURE 11.** Gap of ratio of covered users between Alg-TM. 2 and Alg-DM. 2 with the increased number of WCSs in linear mode.

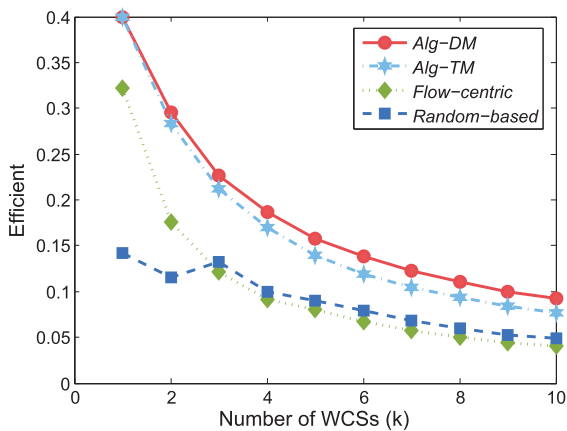


**FIGURE 12.** Coverage efficiency  $\eta$  of each WCS with the increased number of WCSs in linear mode.

acquired by Alg-DM. 2), which is given by  $\psi = |R_2 - R_1|$ . As shown in Fig. 11, we evaluate the gap  $\psi$  by three detouring threshold values  $D = 400m, 800m, 1200m$ . In that, we can see the gap rises with the increased detouring threshold value. This indicates that the improvement acquired by Alg-DM. 2 is significant when increasing coverage range. Lastly but not least, we evaluate the coverage efficiency by selected WCSs.

Based on the ratio of covered users ( $R$ ) and  $k$  WCSs, we introduce a parameter  $\eta$  to describe the average coverage efficiency, which is given by  $\eta = \frac{R}{k}$ . As depicted in Fig. 12, we can see that the average coverage efficiency falls slowly with the increased number of WCSs. This is a proleptic indication which can be got by the diminishing returns rule (submodularity of coverage quality we have proved in Sec. V-C) except the efficiency acquired by Random placement. In that, the efficiency acquired by *random-based* comes from behind by comparing to *flow-centric*. The reason is the same one we have discussed in Fig. 6.

**VII. CONCLUSION AND FUTURE DIRECTIONS**

In this paper, we consider an optimal deployment problem of deploying limited WCSs to maximize the coverage quality with consideration of bounded detouring cost, which should be respected carefully. We convert the deployment problem into the weighted maximum coverage problem, which has been proved to be NP-hard. And we proved the submodularity of objective utility function. After that, threshold mode-driven approximation Alg-TM. 1 is proposed with ratio of  $(1 - \frac{1}{e})$ . By observing the impact of linear/nonlinear mode, we proposed the linear/nonlinear mode-driven Alg-DM. 2 by conducting an improvement in Alg-TM. 1. Finally, the real-world traces validate that our algorithm could outperform coverage quality with 75% comparing to *flow-centric* and *random-based*. In our future work, we would consider the further effects of parameter  $\delta(T_{ij})$  on detouring expectation, which may provide significant impacts different from detouring distance. In addition, the placement budget and the limited recharging service of WCSs should be taken into consideration. We would investigate whether or not the game issue occurs between limited recharging service and serious recharging demands.

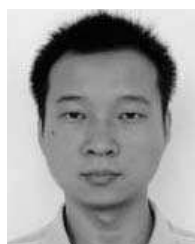
**REFERENCES**

[1] B. Wang, X. Gu, L. Ma, and S. Yan, "Temperature error correction based on BP neural network in meteorological wireless sensor network," in *Proc. Int. Conf. Cloud Comput. Secur.*, 2016, pp. 117–132.  
 [2] Y. Sun and F. Gu, "Compressive sensing of piezoelectric sensor response signal for phased array structural health monitoring," *Int. J. Sensor Netw.*, vol. 23, no. 4, pp. 258–264, 2017.

- [3] J. Shen et al., "A lightweight multi-layer authentication protocol for wireless body area networks," *Future Generat. Comput. Syst.*, 2016.
- [4] G. Anastasi, M. Conti, M. Di Francesco, and A. Passarella, "Energy conservation in wireless sensor networks: A survey," *Ad Hoc Netw.*, vol. 7, no. 3, pp. 537–568, May 2009.
- [5] J. N. Al-Karaki and A. E. Kamal, "Routing techniques in wireless sensor networks: A survey," *IEEE Wireless Commun.*, vol. 11, no. 6, pp. 6–28, 2004.
- [6] W. Ye, J. Heidemann, and D. Estrin, "An energy-efficient mac protocol for wireless sensor networks," in *Proc. IEEE Global Telecommun. Conf.*, vol. 3, Jun. 2002, pp. 1567–1576.
- [7] J.-H. Chang and L. Tassiulas, "Maximum lifetime routing in wireless sensor networks," *IEEE/ACM Trans. Netw.*, vol. 12, no. 4, pp. 609–619, Aug. 2004.
- [8] S. Sudevalayam and P. Kulkarni, "Energy harvesting sensor nodes: Survey and implications," *IEEE Commun. Surveys Tuts.*, vol. 13, no. 3, pp. 443–461, 3rd Quart., 2011.
- [9] A. Kurs, A. Karalis, R. Moffatt, J. D. Joannopoulos, P. Fisher, and M. Soljačić, "Wireless power transfer via strongly coupled magnetic resonances," *Science*, vol. 317, no. 5834, pp. 83–86, 2007.
- [10] *Powercast*. Accessed: Oct. 16, 2017. [Online]. Available: <http://www.powercastco.com/products/powerharvester-receivers/>
- [11] *Powermat*. Accessed: Oct. 16, 2017. [Online]. Available: <https://www.powermat.com/>
- [12] B. Kang and G. Ceder, "Battery materials for ultrafast charging and discharging," *Nature*, vol. 458, no. 7235, pp. 190–193, 2009.
- [13] Y. Shi, L. Xie, Y. T. Hou, and H. D. Sherali, "On renewable sensor networks with wireless energy transfer," in *Proc. IEEE INFOCOM*, Apr. 2011, pp. 1350–1358.
- [14] L. Xie, Y. Shi, Y. T. Hou, W. Lou, H. D. Sherali, and S. F. Midkiff, "Multi-node wireless energy charging in sensor networks," *IEEE/ACM Trans. Netw.*, vol. 23, no. 2, pp. 437–450, Apr. 2014.
- [15] Z. Li, Y. Peng, W. Zhang, and D. Qiao, "J-RoC: A joint routing and charging scheme to prolong sensor network lifetime," in *Proc. 19th IEEE Int. Conf. Netw. Protocols*, Oct. 2011, pp. 373–382.
- [16] L. Fu et al., "Minimizing charging delay in wireless rechargeable sensor networks," in *Proc. IEEE INFOCOM*, 2013, pp. 2922–2930.
- [17] S. Zhang, Z. Qian, F. Kong, S. Lu, and J. Wu, "P<sup>3</sup>: Joint optimization of charger placement and power allocation for wireless power transfer," in *Proc. IEEE Conf. Comput. Commun. (INFOCOM)*, Apr./May 2015, pp. 2344–2352.
- [18] H. Dai, Y. Liu, A. X. Liu, L. Kong, G. Chen, and T. He, "Radiation constrained wireless charger placement," in *Proc. IEEE 35th Annu. Conf. Comput. Commun. (INFOCOM)*, Apr. 2016, pp. 1–9.
- [19] Y. Xiong, J. Gan, B. An, C. Miao, and A. L. Bazzan, "Optimal electric vehicle charging station placement," in *Proc. IJCAI*, 2015, pp. 2662–2668.
- [20] A. Hess, F. Malandrino, M. B. Reinhardt, C. Casetti, K. A. Hummel, and J. M. Barceló-Ordinas, "Optimal deployment of charging stations for electric vehicular networks," in *Proc. 1st Workshop Urban Netw.*, 2012, pp. 1–6.
- [21] J. Walker, *Human Transit: How Clearer Thinking About Public Transit Can Enrich Our Communities and Our Lives*. Washington, DC, USA: Island Press, 2012.
- [22] H. Guo et al., "Modeling the perceptions and preferences of pedestrians on crossing facilities," *Discrete Dyn. Nature Soc.*, vol. 2014, no. 1502, pp. 1–8, Mar. 2014.
- [23] *Mobile Cyber-Physical Systems*. Accessed: Oct. 16, 2017. [Online]. Available: [https://en.wikipedia.org/wiki/Cyber-physical\\_system](https://en.wikipedia.org/wiki/Cyber-physical_system)
- [24] *Maximum Coverage Problem*. Accessed: Oct. 16, 2017. [Online]. Available: [https://en.wikipedia.org/wiki/Maximum\\_coverage\\_problem](https://en.wikipedia.org/wiki/Maximum_coverage_problem)
- [25] A. Krause and C. Guestrin, "A note on the budgeted maximization of submodular functions," *Tech. Rep.*, 2005.
- [26] X. Rao, P. Yang, Y. Yan, G. Liu, M. Zhang, and W. Xu, "Optimal deployment for roadside wireless charger with bounded detouring cost," in *Proc. IEEE Int. Conf. Commun. Workshops (ICC Workshops)*, May 2017, pp. 493–497.
- [27] J. G. Jetcheva, Y.-C. Hu, S. PalChaudhuri, A. K. Saha, and D. B. Johnson. (Sep. 2003). *CRAWDAD Dataset Rice/Ad Hoc City (V. 2003-09-11)*. [Online]. Available: [http://crawdad.org/rice/ad\\_hoc\\_city/20030911/bus\\_mobility](http://crawdad.org/rice/ad_hoc_city/20030911/bus_mobility)
- [28] H. Dai et al., "Impact of mobility on energy provisioning in wireless rechargeable sensor networks," in *Proc. Wireless Commun. Netw. Conf. (WCNC)*, 2013, pp. 962–967.
- [29] H. Dai, Y. Liu, G. Chen, X. Wu, and T. He, "Safe charging for wireless power transfer," in *Proc. IEEE INFOCOM*, Apr./May 2014, pp. 1105–1113.
- [30] S. Nikolettseas, T. P. Raptis, and C. Raptopoulos, "Low radiation efficient wireless energy transfer in wireless distributed systems," in *Proc. 35th IEEE Int. Conf. Distrib. Comput. Syst.*, Jun./Jul. 2015, pp. 196–204.
- [31] L. Chen, S. Lin, and H. Huang, "Charge me if you can: Charging path optimization and scheduling in mobile networks," in *Proc. ACM Int. Symp.*, 2016, pp. 101–110.
- [32] S. Zhang, S. Lu, and J. Wu, "Collaborative mobile charging," *IEEE Trans. Comput.*, vol. 64, no. 3, pp. 654–667, Mar. 2015.
- [33] W. Xu, W. Liang, X. Lin, and G. Mao, "Efficient scheduling of multiple mobile chargers for wireless sensor networks," *IEEE Trans. Veh. Technol.*, vol. 65, no. 9, pp. 7670–7683, Sep. 2016.
- [34] J. Zhang, J. Tang, T. Wang, and F. Chen, "Energy-efficient data-gathering rendezvous algorithms with mobile sinks for wireless sensor networks," *Int. J. Sensor Netw.*, vol. 23, no. 4, pp. 248–257, 2017.
- [35] S. Guo, F. Wang, Y. Yang, and B. Xiao, "Energy-efficient cooperative transmission for simultaneous wireless information and power transfer in clustered wireless sensor networks," *IEEE Trans. Commun.*, vol. 63, no. 11, pp. 4405–4417, Nov. 2015.
- [36] S. Guo, C. Wang, and Y. Yang, "Joint mobile data gathering and energy provisioning in wireless rechargeable sensor networks," *IEEE Trans. Mobile Comput.*, vol. 13, no. 12, pp. 2836–2852, Dec. 2014.
- [37] Y. Xue et al., "A self-adaptive artificial bee colony algorithm based on global best for global optimization," *Soft Comput.*, pp. 1–18, 2017.
- [38] Y. Zhang, X. Sun, and B. Wang, "Efficient algorithm for  $k$ -barrier coverage based on integer linear programming," *China Commun.*, vol. 13, no. 7, pp. 16–23, Jul. 2016.
- [39] H. Lin and J. Bilmes, "A class of submodular functions for document summarization," in *Proc. Conf. Meet. Assoc. Comput. Linguistics, Hum. Lang. Technol.*, Portland, OR, USA, Jun. 2011, pp. 510–520.
- [40] L. Lovász, *Submodular Functions and Convexity*. Berlin, Germany: Springer, 1983.
- [41] H. Zheng and J. Wu, "Optimizing roadside advertisement dissemination in vehicular cyber-physical systems," in *Proc. IEEE 35th Int. Conf. Distrib. Comput. Syst. (ICDCS)*, Jun./Jul. 2015, pp. 41–50.
- [42] M. L. Fisher, G. L. Nemhauser, and L. A. Wolsey, "An analysis of approximations for maximizing submodular set functions—II," *Polyhedral Combinat.*, vol. 8, pp. 73–87, Feb. 2009.
- [43] A. Krause and D. Golovin, "Submodular function maximization," *Tech. Rep.*, 2014, pp. 71–104.
- [44] G. L. Nemhauser, L. A. Wolsey, and M. L. Fisher, "An analysis of approximations for maximizing submodular set functions—I," *Math. Program.*, vol. 14, no. 1, pp. 265–294, 1978.
- [45] S. Khuller, A. Moss, and J. Naor, "The budgeted maximum coverage problem," *Inf. Process. Lett.*, vol. 70, no. 1, pp. 39–45, 1998.



**XUNPENG RAO** received the B.S. degree in information and computing science from the University of Science and Technology, Beijing, China, in 2015. He is currently pursuing the M.S. degree in computer science and technology with the PLA University of Science and Technology, China. His current research interests include wireless energy transfer, wireless rechargeable sensor network, and battery-free sensor network.



**YUBO YAN** (S'10) received the B.S. degree and the M.S. degree in communication and information systems from the College of Communications Engineering, PLA University of Science and Technology, China, in 2006 and 2011, respectively, and where he is currently pursuing the Ph.D. degree. His research interests include cognitive radio networks, software radio systems, and wireless sensor networks.



**MAOTIAN ZHANG** (S'12) received the B.S. degree in communication engineering from Tianjin University, China, in 2011, and the Ph.D. degree in computer science and engineering from the PLA University of Science and Technology, China. His research interests include mobile computing, mobile crowd-sensing networks, and mobile social networks.



**WANRU XU** received the B.S. degree in communication engineering from the PLA University of Science and Technology, China, in 2014, where she is currently pursuing the M.S. degree in computer science and technology. Her research interests include crowdsensing network and mobile advertisement.



**XIAOCHEN FAN** received the B.S. degree from the School of Computer Science and Technology, Beijing Institute of Technology, China, in 2013, and the M.S. degree from the College of Communication Engineering, China, in 2016. He is currently pursuing the Ph.D. degree with the School of Computing and Communications, Faculty of Engineering and Information Technology, University of Technology, Sydney, Australia. His research interests include mobile cloud computing, wireless networking, and crowdsensing networks. He is a Student Member of the IEEE Computer Society.



**HAO ZHOU** (M'15) received the B.S. and Ph.D. degrees in computer science from the University of Science and Technology of China, Hefei, China, in 1997 and 2002, respectively. He was a Project Lecturer with the National Institute of Informatics, Japan, from 2014 to 2016. He is currently an Associate Professor with the University of Science and Technology of China. His research interests include software engineering, protocol testing, and wireless networking.



**PANLONG YANG** (M'02) received the B.S., M.S., and Ph.D. degrees in communication and information system from the Nanjing Institute of Communication Engineering, China, in 1999, 2002, and 2005, respectively. He is currently a Professor with the College of Computer Science and Technology, University of Science and Technology of China. His research interests include wireless mesh networks, wireless sensor networks, and cognitive radio networks. He is a member of the IEEE Computer Society and the ACM SIGMOBILE Society.

...